Coefficient Selection Algorithm a Two Stages Image Fusion Method Based on Wavelet Transform

Miguel Archanjo Bacellar Goes Telles jr, Antonio Nuno de Castro Santa Rosa and Paulo Quintiliano

Abstract— Image fusion consists of an advanced set of digital image processing techniques, which are used to combine images of different sensors. The main objective is to obtain a synthetic image that gathers the best qualities of each original image. This paper presents a new image fusion method based on selection of coefficients that takes into account the image fusion from sensors of either different or same satellites. The method is based on wavelet transform and multiresolution analysis. It separates fusion and resampling in different stages, allowing the use of different filters or bases of wavelet transform, in each one of them, in order to get better results. The advantage of the image fusion is to join the best spatial resolution of an image with spectral data of other image in a synthetic one. The results obtained with this method allow us to infer that the synthetic image produced has better spectral and spatial quality than IHS.

***Index Terms*— image fusion, image processing, remote sensing, wavelets.**

I. Introduction

This paper presents the image fusion with Coefficient Selection Method (CSA) [1]. The method is a variation of those methods that use wavelet transform (WT) and the multiresolution analysis (MRA). It separates fusion and resampling in two different stages and allows the use of the different filters in each stage. First, the fusion stage uses an algorithm to calculate the ratio between the images to be fused, i.e. the high spatial resolution image (HSRI) and the low spatial resolution image (LSRI). Secondly, the resampling stage uses another algorithm to compensate the loss of spectral information on the pixels of the edges of the image, since most of the edge information of the synthetic image that comes from the HSRI and not from LSRI. Finally, the results obtained with the fusion by the CSA method are compared with the results obtained with the fusion of the same images using the Intensity-Hue-Saturation method (IHS).

The methods based on WT and MRA are common in the image fusion literature. They have been studied at least for one decade, which stand out their studies in the processes of selecting filters coefficients, scale levels, and type of sensors to be used [2]-[6].

The application of WT in digital image processing is a natural consequence of the evolution of the methods based on spectrum of frequency analysis obtained through a transform. The computational treatment of WT is made through algorithms that operate on data in different scales or resolutions.

According to [3], the synthetic image resultant of the fusion depends on the wavelet base used.

To accomplish the image fusion it is necessary that all images are under the same coordinate system, or they have been preprocessed in such a way that they represent the same geographic area, called registration. The registration error should be smaller than a pixel.

The registration superimposes two or more images of a same scene. The registered image is called reference image, and the other is called adjustment image [7]. This process is accomplished in such a way that the coordinates of a point in each image corresponds to the same geographical space [8]. After the images are superimposed math operations are done in each pixel. There are factors that may influence the quality of the image fusion, such as: acquisition date, weather conditions and illumination which facilitate, restrict or obstruct the processing, combined or isolated.

As the fusion always happens among two images, and one is a LSRI and the other HSRI. We generalized the term panchromatic referring to images of higher spatial resolution. Panchromatic image is barely available for a scene that is going to be fused. A multispectral band of a sensor with high spatial resolution could be used to accomplish of image fusion processing.

This paper is structured in six sections. Section II, a brief overview of WT and MRA theory; section III, concepts of

M. A. B. G. Telles Jr., is with Image and Geographic Information a Branch of Terrestrial Command of Brazilian Army, Centro Universitário de Brasilia – UniCEUB and Geosciences Institute of University of Brasilia - UnB , Campus Universitário Darcy Ribeiro, ICC-Sul, IG, 70910-000, Brasilia – DF, Brazil (e-mail: archanjo@unb.br).

A N C Santa Rosa, is with Sistema de Proteção da Amazônia – SIPAM and the Geosciences Institute of Brasilia University - UnB , Campus Universitário Darcy Ribeiro, ICC-Sul, IG, 70910-000, Brasilia – DF, Brazil (e-mail: nunos@unb.br).

P.Q, is with Brazilian Federal Police, Brazilian Federal Police, SAIS Quadra 7, Lote 21, Ed. INC/DPF, Brasília-DF, Brazil (quintiliano.pqs@dpf.gov.br).

image fusion and the classifications of different fusion levels are presented; section IV, details of the CSA method; section V, results obtained by the CSA and IHS method are compared with each other. Finally, section VI, conclusions about CSA method.

II. Wavelet Transform and multiresolution analisys

WT has been in use in digital imaging processing applications since late 80`s.

The WT using the pyramid algorithm allows the MRA [9]. This is how it works, the processing builds images with resolution that differs from theirs originals [10]. This construction reaches a level that allows changing of information between the images that are being fused or math operations between them. The images that are on the top of the pyramid are the ones with largest level of details or larger resolution when compared with the original, while copies of lower level of details or smaller resolution are on the bottom of the pyramid. It's knew as reverse pyramid.

There are three types of pyramidal images: a low-pass, a band-pass and a wavelet pyramid [10]. The wavelet is the most used and it can be defined as a type of band pass filter, with the difference of storing the details of the image separately by means of the horizontal (LH), diagonal (HH) and vertical details (HL). The image's spectral information is stored in approximation coefficients (LL). Details or edges in images are simple and connected contours, one pixel thickness, placed in the center of two adjacent areas with a considerable difference between its gray levels [11]. The details images are the representation of the edges, in each directions obtained by the WT.

The WT capability allows one to differentiate image parts represented in different resolutions [10]. The WT handles different parts of image appropriately. Besides posses compact support, the wavelets contains also the following characteristics: number of pixels of the transform match the image and the transform is a recursive structure, with tree level's resolution.

The Continuous WT is obtained by the dilatation and translation properties in a prototype of a base function. With that, we obtain both continuous and orthonormal wavelet functions, where the dilations and translations defined by two variables *a* and *b*, respectively (1).

$$\Psi_{a,b}(t) = \frac{1}{\sqrt{a}} \Psi\left(\frac{t-b}{a}\right). \quad (1)$$

The series and discrete wavelet transform will be defined as:

$$f(t) = \sum_{m\to-\infty}^{\infty} \sum_{n\to-\infty}^{\infty} \left\langle f, \Psi_{m,n} \right\rangle . \Psi_{m,n}(t) = \sum_{m\to-\infty}^{\infty} \sum_{n\to-\infty}^{\infty} C_{m,n} . \Psi_{m,n}(t). \quad (2)$$

Keeping in mind that human perception of the universe uses a scale concept, where each accomplished observation is made in an adapted scale for understanding necessary different details. Based on this concept, one can build families of discrete wavelets and develop fast algorithms for the transform calculation.

The resolution levels are described under the form of a nested of function spaces, where each space with higher resolution contains spaces with smaller resolution, as expressed below:

$$\ldots \subset V_{-2} \subset V_{-1} \subset V_0 \subset V_1 \subset V_2 \subset \ldots \quad (5)$$

Bidimensional WT of an image is obtained by applying the transform to the image's columns and then to the lines. That is possible because the WT is a unitary transformation. It means that, the bidimensional transform becomes separable falling in the unidimensional transform case for each dimension of the image, i.e. it's columns and lines.

III. Image Fusion

Image fusion is defined as the combination of two or more different images to form a new one, through the use of an algorithm [12].

The data fusion is classified on three levels: pixel level, feature level and decision level. Details of the data fusion classification levels is obtained in [13]-[14].

Image fusion at pixel level means to process it in the lowest processing level corresponding to the fusion of physical parameters of the image. In the pixel level, data in raster format must be registered or georreferenced. An image with significant errors of registration usually leads to bad interpretation, appearance of false colors and artificial features at the end of the fusion process. The registration includes the resampling of the image to a new spacing between the pixels and new projection. Comparison between the methods of geometric correction can be obtained in [15]-[16].

The geometric correction aims assure that the images to be fused represent the same geographic region, independent of the acquisition from different sensors or they possess different spatial resolutions.

The pixel level is the most developed method and contains three fusion methods, as follows [14]:

- Color transformation, as in, fusion with the IHS method;
- Numeric and statistical methods, as in, analysis of principal components; and
- multiresolution analysis.

These methods processes image fusion using arithmetic procedures, substitution components techniques such as Intensity-Hue-Saturation (IHS) and Principal Components (PCA) [17]-[19]. Nevertheless, those methods might lead to significant distortion of radiometric resolution of the synthetic image, They produce high quality images for visual interpretation, because of texture enhancement

The radiometric correction consists of adjusting brightness and contrast of HSRI, with the brightness and contrast of the LSRI bands. It is necessary, because the quality of the fusion is directly dependence of the high correlation issue between the images [21].

The objective of fusing HSRI with contains high spatial resolution and LSRI, which contains high spectral resolution, is to increase the image details and preserve spectral information. This is useful for applications based on spectral signature.

IV. THE COEFFICIENT SELECTION ALGORITHM

The CSA is an algorithm method designed as an image fusion method that provides tools to fuse images from different sensors, spatial and spectral resolution. It can accomplish in two stages called fusion and resampling. The aim of separate the method in two stages is: 1) It allows the use of either different or same filters (wavelet bases), in each stage; Using different fusion algorithms, as explained below, in the fusion stage; and 2) The use of different levels of decomposition by WT in each stage. In contrast ,image fusion methods, like IHS, that require the selection of spectral bands before the fusion, while methods based on WT, generally requires one band at a time, i.e., each spectral band must be fused with HSRI band separately. Therefore, WT based methods are more flexible. The CSA method uses a decimated WT (DWT) and MRA. Details about decimated and undecimated WT can be obtained in [22] and [23].

A. Fusion stage

The fusion stage is based on analysis of the methods [2]-[6]. It was verified that those methods execute in one stage the fusion and the resampling of the image. Disadvantages of having fusion and resampling in only one stage are: 1) only one filter can be used for fusion and resampling; and 2) the levels of decomposition of the image by the WT are fixed with base in a ratio between the images, meaning that one cannot choose in which level to fuse and in which level to resample.

Before images can be fused they must be evaluated as the ratio between its lines and columns. That is done to verify if the ratio between them is a power of 2 and if it is not, a resampling of the image is made to reach the closest power of 2, using the nearest neighbor interpolator (6).

$$\eta L_{new} = \frac{\eta L_{pan}}{2^{\text{int}(\log_2 \frac{2\eta L_{pan}}{\eta L_{old}})}}, \quad (6)$$

Where:

ηL_{pan} is the number of lines in HSRI;

ηl_{old} is the number of lines in LSRI before interpolation; and

ηl_{new}, is the number of lines of LSRI after interpolation.

In the same way for the columns we have:

$$\eta C_{new} = \frac{\eta C_{pan}}{2^{\text{int}(\log_2 \frac{2\eta C_{pan}}{\eta C_{old}})}}, \quad (7)$$

Where:

ηC_{pan} is the number of columns in HSRI;

ηC_{old} is the number of columns in LSRI before interpolation; and

ηC_{new}, is the number of columns in LSRI after interpolation.

The fusion stage is divided in three phases: decomposition, sum of subbands and fusion properly said.

First, the decomposition of image consists in obtaining the subbands LL, LH, HL and HH by WT and MRA, in a level where all the involved subbands have the same size. Second, the sum of subbands (8) is used as an intermediary stage fusion, and its objective is to enrich the subband LL of the LSRI, with the details coefficients of the subbands LH, HL and HH of HSRI through a direct sum of them. The summation will produce an image IM_A, with spectral information and details similar to those in the HSRI.

The methods based on sum of coefficient were first proposed by [3] and more information about these methods can be obtained in [24].

$$IM_A = (LL_{LRSI}) + (HL_{HRSI} + LH_{HRSI} + HH_{HRSI}), \quad (8)$$

Where:

LL_{LRSI} : Subband of approach of the LSRI;

HL_{HRSI} : Subband of vertical details of the HSRI;

LH_{HRSI} : Subband of horizontal details of the HSRI; and

HH_{HRSI} : Subband of diagonal details of the HSRI.

Third, the fusion is made by starting from the image IM_A and LSRI. In this stage the images have the same dimensions and are decomposed in the fusion level l_{Fusion}. In this level, an algorithm is used to select coefficients between the LL subbands of IM_A and LSRI.

The simplest algorithm to select coefficients is the substitution of the subband LL of IM_A by the subband LL of the LSRI. The algorithms tested and implemented in the CSA method are: minimum, maximum, absolute minimum, absolute maximum and the selection coefficients algorithms from [2] and [20]. They are used to select among the subbands LL of the IM_A and LSRI, which coefficient will be selected to form a new LL subband. After an algorithm is chosen to select the coefficients, the subbands are processed using inverse wavelet transform (IWT) and the synthetic image IM_F is obtained finishing the fusion stage. The whole fusion process is presented in the fig. 1, and described below:

a) The process begins with the registration of the images;

b) A scale algorithm is used to verify the ratio between the images. When the ratio between them are different from a power of 2, the nearest neighbor interpolator algorithm is used to achieve it;

c) the images are decomposed through WT to the level of the sum of subbands;

d) The subband LL of the LSRI replaces the subband LL of the HSRI;

e) The algorithm sum of subbands (8) is used then in the bands of details and approach of the HSRI, resulting in the image IM_A;

f) Both the image IM_A and the LSRI are decomposed through WT at the fusion level. In this stage, the subband LL of the LSRI replaces the subband LL of the image IM_A; and

g) Next, we use one of the implemented algorithms to select coefficients of subband LL among IM_A and the LSRI;

h) IWT is used to reconstruct the image IM_A, which results in image IM_F.

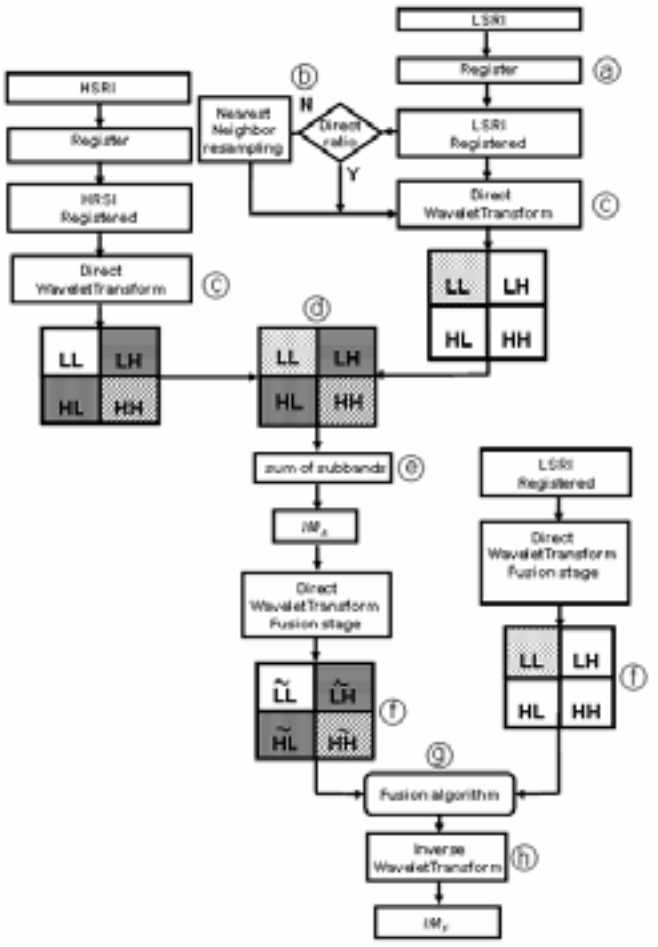

Fig. 1 - Stage fusion diagram.

B. Resampling Stage

It is necessary that both histograms of HSRI and LSRI be adjusted. This adjustment may approach the values of the mean and variance by giving them same center and spread.

The resampling by WT is accomplished decomposing the adjusted HSRI and the image IM_F, in the resampling level l_R. It is the smallest useful level that can be used. Although, larger levels than l_R can be used. Once the images have been decomposed, the substitution of subband LL of the adjusted HSRI by the subband LL of IM_F is done. After that, the Addition Algorithm With Color Compensation Factor (AAWCCF) is used, as proposed by [6], for the selection of details coefficients of IWT. The value of each coefficient in the reconstruction is calculated by the equation (8), as follows:

$$d_j^S = \max(d_j^{XS}, d_j^P) + (1 - k_j) d_j^{XS} \quad (9)$$

Where:

d_j^S are the coefficients of the subbands of details of the S synthetic images in the level j;

d_j^{XS} are the coefficients of the subbands of details of the LSRI;

d_j^P are the coefficients of the subbands of details of the HSRI; and

$(1-k_j)$ is the color compensation factor, where k_j is the correlation coefficient (CC) among the subband LL of both images in the level j.

The AAWCCF is used to allow that some details coefficients of the LSRI be introduced in the synthetic image, to compensate the loss of spectral information on the edges of that image. The details coefficient of the LSRI and adjusted HSRI are inserted in IM_F, based on its color compensation factor. As smaller the factor is, more details of the LSRI is used. The algorithm also allows more details of the adjusted HSRI be inserted without loss of the spectral information.

Synthetic reconstruction, of the image is obtained with spatial resolution of the original HSRI and spectral information of the LSRI band.

Step-by-step decryption of the resampling stage showed in the fig. 2 is described below:

a) The resampling begins with the adjustment of the mean and the variance of the HSRI with the LSRI band that will be fused;

b) The images are decomposed at the resampling level through WT;

c) After decomposition, the substitution of the subband LL of the adjusted HSRI by the subband LL from IM_F is made;

d) The AAWCCF is used to compensate the loss of spectral information at the edges;

e) IWT is used to reconstruct the synthetic image; and

f) After the processing of IWT, the synthetic image is obtained.

The presented method follows the ARSIS concept as proposed by [25].

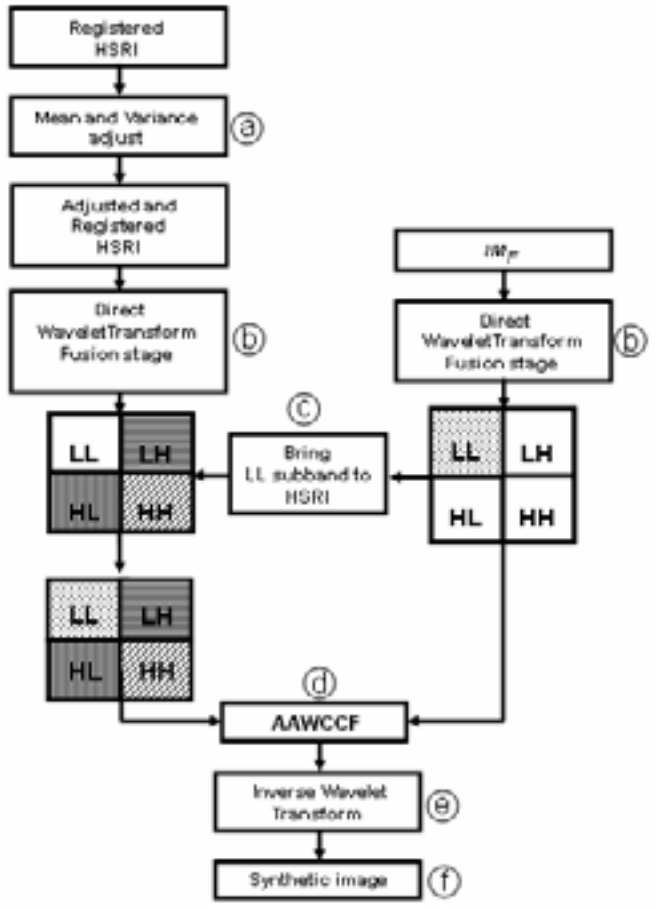

Fig. 2 – Resampling Stage Diagram.

V. Cases of Image Fusion with CSA and IHS

This section explores case which are part of the set of tests developed to evaluate the results of CSA method. Besides that, others were accomplished with images from the satellites: SPOT5, Landsat 7, Quickbird and Radarsat.

Image fusion Landsat 5 and IRS-1C

Here the image fusion uses TM and Panchromatic sensors. The multispectral bands used with 30 meters of spatial resolution are from Landsat 5 satellite and the HSRI with 5 meters of spatial resolution is from IRS-1C satellite. The images are of the city of Anápolis - GO, Brazil, and they were acquired on June 8th and 9th, 1999, respectively. The spectral intervals of the bands used are showed in fig. 3.

The levels of decomposition used in the fusion and resampling stages were 3 and 4, respectively. The filters used were proposed by [26].

The fig. 4 (a) presents the original TM543 image. For the presentation of the results, due to size restrictions, sub areas of the HIS fig. 4 (b) and synthetic images fig. 4 (c) were selected.

For the comparison between the proposed fusion process and the IHS method, the original LSRI was resampled to the spatial resolution of the original panchromatic image, which had its histogram adjusted to each of LSRI bands.

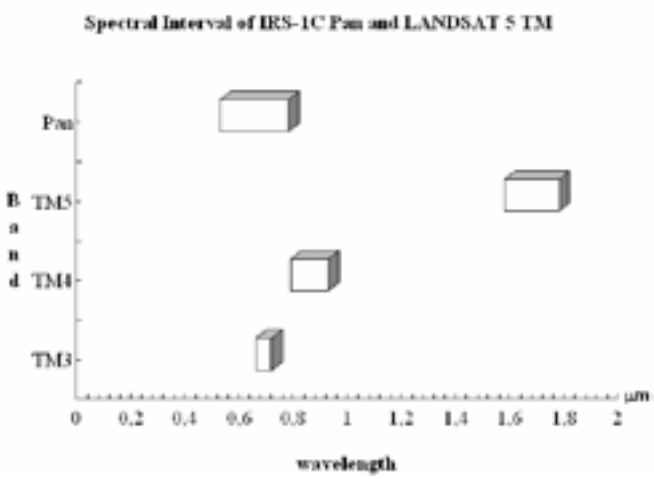

Fig. 3 – Spectral interval of the images IRS-1C and Landsat 5.

As result, in fig. 4 (b) and 4(c) we see the images fused by IHS and CSA, respectively. The IHS image has a variation in the spectral response when compared with the original LSRI. The spectral response of the targets presented in the image, in general, was attenuated. The synthetic image had a variation in its contrast; its spectral response is better than in the IHS image as we can see with the statistics of both images showed in table II. Both images have a variation in contrast. This is due to the fact of the bands 5 and 4 of TM sensor be out of IRS-1C spectral interval. This leads to a lack of correlation between TM bands and HSRI even after the histogram adjustment.

Fig. 5 presents details of the LSRI, synthetic image and HSRI. As one can see in Fig. 5(a), some details of the airfield have problems in its edges, probably associated to the acquisition or to the preprocessing of the original image. On fig. 5(b), the problem is solved, due to the prevailing HSRI detail information. Fig. 5(c) presents the comparison of the edges preserved in the synthetic image when compared to Fig. 5(d), that corresponds to a cut in the panchromatic image. Fig. 5(e) and 5(f) presents the preservation of the details (edges) in a not very populated area. Fig. 5(g) twice increased, presents a cut of the original TM543 image of the area presented on figs. 5(e) and 5(f). At closer look the contrast was not very altered by image fusion.

In conclusion, as presented in table I there is a high correlation between the data. The smallest correlation in the band 4 happens because the predominant target, in the scene, is an urban area, which possesses low spectral response in this band. The other bands show a better correlation because they present better spectral response to the targets of the scene. In the case of urban areas, bands 3 and 5 have high responses, better in the latter case. Vegetation presents a smaller answer in the band 3 than in bands 4 and 5, namely that the predominant target in the scene is the urban area.

(a)

(b)

(c)

Fig 4 - original TM543 image (a), TM 543 fused by IHS method (b) and Synthetic IRS1-C/TM543 (c).

(a)

(b)

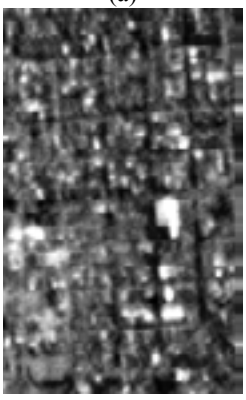

(c)

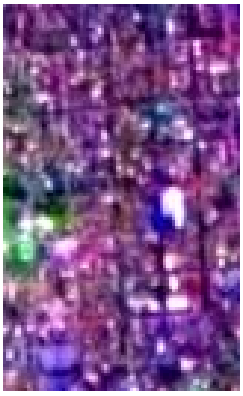

(d)

(e)

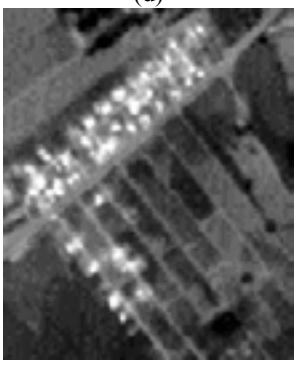

(f)

(g)

Fig 5- Details of images, (a) details of airfield on the LSRI image with acquisition or preprocessing problems, (b) the problem was solved by the fusion process, (c) a cut of original HSRI image, (d) a cut of the synthetic image, (e) and (f) shows agricultural field on Synthetic and HSRI images, respectively, (g) a cut of original LSRI image, the same area of (e) and (f).

TABLE I
Statistics of Images on Fusion Stage

Band	CC	Mean	Std. Dev.
TM5	1.00	78.05	17.71
Fused_5	0.70	77.86	18.08
TM4	1.00	46.23	9.21
Fused_4	0.06	46.30	9.97
TM3	1.00	33.72	11.29
Fused_3	0.60	33.79	12.10

In table II statistics for images on fusion stage are summarized. As it can see, the results of CSA are better than IHS. CC, mean and standard deviation values, when compared, ratifies our evaluation. The statistics of synthetic image is better than IHS image in all cases, specially when the LSRI band is out of the spectral interval of the HSRI.

TABLE II
Statistics of Images on Resample Stage

Band	CC	Mean	Std. Dev.
TM3_resampled	1.00	33.72	11.30
Synthetic_3	0.79	33.42	12.63
IHS_TM3	0.78	47.38	33.89
Pan_TM3	0.74	33.22	11.41
TM4_resampled	1.00	46.24	9.21
Synthetic_4	0.67	50.71	10.89
IHS_TM4	0.27	59.21	30.32
Pan_TM4	0.03	50.90	11.23
TM5_resampled	1.00	78.05	17.71
Synthetic_5	0.68	85.04	21.15
IHS_TM5	0.56	103.61	56.32
Pan_TM5	0.54	84.73	22.64

VI. Conclusion

The largest problem in the accomplishment of image fusion, using methods based on WT and MRA, consists on the search of the best bases or filters to be used. There is not only one optimal base and scale factor and the difference of spectral interval between the bands used in the fusion is a factor that has a great influence in the final result.

The images used in this study presented different: spectral intervals, spatial resolutions, dates and acquisition geometries, and they demonstrate the flexibility of the CSA method in processing different remote sensing images.

The division of the method, in two stages, brought the benefit of accomplish the fusion and resampling in different levels, independent to each other, as well as the use of different bases (filters) for each of those stages.

The scale algorithm and WT allow a most precise use of the nearest neighbor interpolator, Since the presented method does not resample LSRI to the same size of HSRI as made in [2]-[5].

The analysis of the results allows us to conclude that:

- The proposed method preserves the spectral information better than IHS method;
- In the IHS method, there is a loss of spectral resolution, mainly for the bands not included in the spectral interval of the HSRI;
- The synthetic image produced by the CSA method presents the same dimensions of HSRI; it doesn't happen with the IHS method.

Now we are studying the à trous wavelet transform, that consists of the application of the non decimated wavelet transform and using as resampling algorithm the direct cosine transform - DCT. The first results are promissing.

Therefore, the accomplished experiments demonstrated the wide possibilities of the application of synthetic images produced by the proposed method in an array of activities such as environmental surveying, defense, cartography, geological surveying, vegetation analysis, urban occupation and forensic. The last one in a wide area of forensic applications.

References

[1] M. A. B. G Telles Jr, A. N. C. Santa Rosa. “Image Fusion Using Addition of Subband Method Based on Wavelet Transform”, In *Proc of*: *PRIP'05 Eighth International Conference on Pattern Recognition and Information Processing, 2005*, Minsk, v. 1, p.150-159, 2005.

[2] H. Li, B. S. Manjunath, S. K. Mitra, “Multisensor image fusion using the wavelet transform”, *Graphical Models and Image Processing,* vol. 57, n. 3, pp. 235-245, 1995.

[3] D.A Yocky, “Multiresolution wavelet decomposition image merger of Landsat Thematic Mapper and SPOT panchromatic data”, *Photogrammetric Engineering & Remote Sensin*g, v. 62, n. 9, p. 1067-1074. 1996.

[4] T. Ranchin, L. Wald, M. Mangolini, “The ARSIS method: a general solution for improving spatial resolution of images by the means of sensor fusion”, in *Proc. of the Conference on Fusion of Earth data: merging point measurements, raster maps and remotely sensed images*. p. 53-59. 1996.

[5] B. Garguet-Duport, J. Girel, J. Chassery, G. Pautou, “The use of multiresolution analysis and wavelets transform for merging SPOT panchromatic and multispectral image data”. *Photogrammetric Engineering & Remote Sensing,* Vol. 62, n. 9, pp. 1057-1066, Sep. 1996.

[6] F. N. Ventura, L. M. G Fonseca, A. N. C Santa Rosa, “Remotely sensed image fusion using the wavelet transform”. In *Proc of* International Symposium on Remote Sensing of Environment, 4 p. (CD-Rom), Buenos Aires, 2002.

[7] L. M. G. Fonseca, B. S. Manjunath, “Registration techniques for multisensor remotely sensed imagery”. *Journal of Photogrammetry Engineering & Remote Sensing*, Vol. 62 (9), pp. 1049-56, Sep. 1996.

[8] C. Pohl, H. Touron, “Operational applications of multi-sensor image fusion”, *International Archives of*

Photogrammetry and Remote Sensing. Vol. 32, pp.123-127, 1999.

[9] S. Mallat, "A Theory form multiresolution signal decomposition: the wavelet representation". *IEEE Transactions on Pattern Analysis and Machine Intelligence*, v.11, n. 7, pp. 674-693, 1989.

[10] A. Watt, F. Policarpo, The Computer Image, New York: Addison-Wesley, 1998.

[11] L. J. V. Vliet, I. T. Young, A. L. D. Beckers, "An edge detection model based on nonlinear Laplace filtering". Pattern Recognition and Artificial Intelligence, E.S. Gelsema and L.N Kanal (eds), Elsevier Science Publishers B.V., North-Holland, pp. 63-73, 1988.

[12] C. Pohl, J. L. Genderen, "Multisensor image fusion in remote sensing: concepts, methods and applications". *International Journal of Remote Sensing*, vol. 19, n. 5, pp.823- 854, 1998.

[13] L. Wald, "Definitions and terms of reference in data fusion". *International Archives of Photogrammetry and Remote Sensing*, v. 32, part 7-4-3, W6, 1999.

[14] W. Chao, Q. Jishuang, L. Zhi, "Data fusion, the core technology for future on-board data processing system". *International Society for Photogrammetry and Remote Sensing*, *Future Intelligent Earth Observing Satellites - FIEOS 2002 Conference Proceedings*, Denver, 2002.

[15] P. Cheng, T. Toutin, C. Pohl, "A Comparisson of geometric models for multisource data fusion", in *Proc. of International Symposium GeoInformatics '95*, Hong Kong, pp. 11-17, 1995.

[16] T. Toutin, "Multisource data integration with an integrated and unified geometric modeling". In *Proc. of 14th EARSeL Symposium on Sensors and Environmental Applications*. Goteborg, pp.163-174, 1994.

[17] W. J. Carper, T. M. Lillesand, R. W. Kiefer, "The use of intensity-hue-saturation transformations for merging SPOT panchromatic and multispectral image data". *Photogrammetric Engineering & Remote Sensing*, v. 56, n. 4, pp. 459-467, 1990.

[18] A. P. Crosta, "Processamento digital de imagens de sensoriamento remoto", UNICAMP, ed. Ver.Campinas, 1992.

[19] V. K. Shettigara, "A generalized component substitution technique for spatial enhancement of multispectral images using a higher resolution data set". *Photogrammetric Engineering & Remote Sensing*, v 58, n. 5, pp.561-567, 1992.

[20] P.J. Burt, R.J, Kolczynski, Enhanced image capture through fusion. In *Proc of* 4th Intl. Conference on Computer Vision, 173-182, 1993.

[21] R. A. Schowengerdt, Remote Sensing: models and methods for image processing. New York: Academic Press. 1997. 523 p.

[22] B. Aiazzi, L. Alparone, S. Baronti and A. Gazelli, "Context-Diven fusion of high spatial and spectral resolution images based on oversampled multiresolution analysis", IEEE Trans. Geosci. Remore Sens., vol. 40, no. 10, pp. 2300-2312, Oct 2002.

[23] X. Otazu, M. Gonzales-Audícana, O. Fors, and J. Núñez, "Introduction of sensor spectral response into image fusion methods. Aplication to wavelet-based methods", IEEE Trans. Geosci. Remore Sens., vol. 43, no 10, Oct 2005.

[24] J. Núñez, X. Otazu, O. Fors, A. Prades, V. Palà, and R. Arbiol, "Multiresolution-based image fusion methods with additive wavelet decomposition", IEEE Trans. Geosci. Remore Sens., vol. 37, no. 3, May 1999.

[25] T. Ranchin, B. Aiazzi, L. Alparone, S. Baronti, L. Wald, "Image fusion-the ARSIS comcept and some successful implementation schemes", ISPRS Journal of Photogrammetry and Remote Sensing, vol. 58, pp. 4-18, 2003.

[26] C. CHEONG, K. AIZAWA, T. SAITO, M. HATORI, "Subband image coding with biorthonormal wavelets", *EICE Trans. Fundamentals of Eletronics, Communications and Computer Sciences*. pp. 871-881. 1992.

Miguel Archanjo Bacellar Goes Telles Jr. The dipl. Telecomunicações from Estácio de Sá University, Rio de Janeiro, Brazil, in 1989, the specialization in Systems Analysis from Veiga de Almeida University, Rio de Janeiro, Brazil, in 1991, The M. Sc. in Computer Science from University of Brasilia – UnB, Brasilia, Brazil, in 2003, and he is currently pursuing the Ph.D. degree in Geology.

He is currently student of Ph.D. program of Geoscience Institute of University of Brasilia – UnB. he is Captain of Brazilian Army and works with remote sensing, GIS and imaging processing, with Image and Geographic Information Branch of Terrestrial Command of Brazilian Army, Brasilia –DF, Brazil. His research interests include image fusion, superresolution, remote sensing and GIS.

Antonio Nuno de Castro Santa Rosa. Received the B.S. degree in Mathematics from Federal University of Pará (UFPA), Brazil, in 1984, the M.Sc. degree in Geophysics from Federal University of Pará (UFPA), Brazil, in 1989, The Ph.D. degree in Geophysics from Federal University of Pará (UFPA), Brazil, in 1996, Post Doctoral degree in Applied Computing from National Institute for Space Research (INPE), Brazil, in 2002.

He is currently Researcher and Professor at Geosciences Institute at University of Brasilia. He is leader of Automatic Image Interpretation Group of National Research Council - CNPq.

interests include image fusion, superresolution, remote sensing and GIS.

Paulo Quintiliano is B.S. degree in Computer Science and Law, M. Sc. in Computer Science from University of Brasilia – UnB, Brasilia, Brazil, in 2001, The PhD in Image Processing and Pattern Recognition from University of Brasilia – UnB, Brasilia, Brazil, in 2001.

He is currently Criminalist - Forensic Computer Crime Unit of Brazilian Federal Police. His research interests include: Image Processing, Pattern Recognition and forensic computing.